Journal of Colloid and Interface Science 585 (2021) 148–157

Contents lists available at ScienceDirect

Journal of Colloid and Interface Science

journal homepage: www.elsevier.com/locate/jcis

Regular Article

Congener-dependent conformations of isolated rhamnolipids at the vacuum-water interface: A molecular dynamics simulation

Stephen R. Euston [a,*], Ibrahim M. Banat [b], Karina Salek [a]

[a] Institute of Mechanical, Process and Energy Engineering, School of Engineering and Physical Sciences, Heriot-Watt University, Edinburgh EH14 4AS, UK
[b] School of Biomedical Sciences, University of Ulster, Coleraine BT52 1SA, UK

GRAPHICAL ABSTRACT

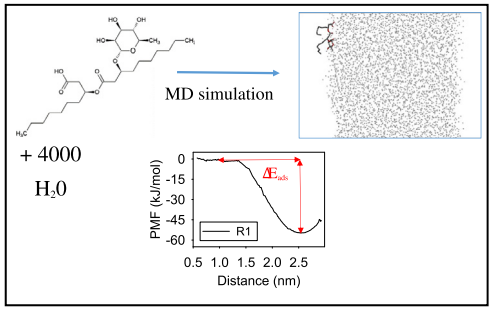

ARTICLE INFO

Article history:
Received 11 June 2020
Revised 20 November 2020
Accepted 21 November 2020
Available online 26 November 2020

Keywords:
Rhamnolipid
Biosurfactant
Molecular dynamics
Adsorption
Vacuum-water interface

ABSTRACT

Hypothesis: Molecular dynamics simulation can be used to differentiate between the adsorption properties of rhamnolipid congeners at a vacuum-water interface.
Experiments: Adsorption of five congeners with differing alkyl chains (two C10 chains, two C14 chains or mixed C14C10 and C10C14), number of rhamnose rings (mono- or di-) and carboxyl group charge (non-ionic or anionic) are simulated at the vacuum-water interface.
Findings: All rhamnolipids adsorb in the interfacial region with rhamnose and carboxyl groups closer to the water phase, and alkyl chains closer to the vacuum phase, but with differing adsorbed conformations. Headgroups of uncharged congeners show two preferred conformations, closed and partially open. Di-rhamnolipid has a low proportion of closed conformation, due to the steric constraints of the second pyranose ring. Charged congeners show strong preference for closed headgroup conformations. For rhamnolipids with equal alkyl chains lengths (C10C10, C14C14) the distribution of alkyl chain tilt angles is similar for both. Where chain lengths are unequal (C14C10, C10C14) one chain has a greater tendency to tilt towards the water phase (>90°). The order parameter of the alkyl chains shows they are disordered at the interface. Together, these results show congener-dependent adsorbed conformation differences suggesting they will have differing surface-active properties at vacuum-water and oil-water interfaces.

1. Introduction

Many surfactants that are in current use in industry are made by chemical synthesis from petrochemical feedstock. With the drive towards reducing dependence on oil-derived chemicals, and the

Abbreviations: R1, L-rhamnosyl-β-hydroxydecanoyl-β-hydroxy decanoate; R2, L-rhamnosyl-L-rhamnosyl-β-hydroxydecanoyl-β-hydroxydecanoate; C14C14, L-rhamnosyl-β-hydroxytetradecanoyl-β-hydroxy tetradecanoate; C14C10, L-rhamnosyl-β-hydroxytetradecanoyl-β-hydroxy decanoate; C10C14, L-rhamnosyl-β-hydroxydecanoyl-β-hydroxy tetradecanoate.

* Corresponding author.
E-mail address: S.R.Euston@hw.ac.uk (S.R. Euston).

https://doi.org/10.1016/j.jcis.2020.11.082
0021-9797/

negative perception of synthetic chemical additives (particularly in consumer products) among the general public, there is desire to replace these with natural counterparts. Biosurfactants, and in particular those produced by microorganisms such as bacteria and fungi, are receiving ongoing attention as potential replacers of chemically derived surfactants [1]. As well as being perceived as natural, they also often have the advantage of being more easily biodegraded, sustainable, less toxic and with equivalent surface activity to synthetic surfactants [2]. The most common types of biosurfactant produced by microorganisms are the glycolipid surfactants such as rhamnolipids, sophorolipids and mannosylerythritol lipids [3].

Rhamnolipid biosurfactants, in common with other glycolipids, contain a hydrophilic head group, in this case rhamnose sugars, and a lipid tail, which in rhamnolipids is comprised of β-hydroxyalkanoic acid chain. The most common rhamnolipids congeners are the mono-rhamnolipid L-rhamnosyl-β-hydroxydeca noyl-β-hydroxydecanoate (R1), with one rhamnopyranose ring and two unsaturated C10 alkyl chains, and the di-rhamnolipid equivalent L-rhamnosyl-L-rhamnosyl-β-hydroxydecanoyl-β-hydro xydecanoate (R2) with two rhamnopyranose rings and two C10 chains [4] (Fig. 1).

The surface active and solution properties of rhamnolipids are properties of technological importance in industry. Surface properties of surfactants determine their ability to adsorb to surfaces and act as emulsifying and foaming agents and lubricants. In solution, surfactants (including rhamnolipids) can form various structures such as micelles, vesicles, bilayers and various mesophases that are important in applications such as encapsulation and structure formation in foods [5]. The formation of micelles in solution of rhamnolipids and glycolipids in general have been studied experimentally, and information has been inferred about the structure of such micelles. In dilute solution, glycolipids are able to self-associate into spherical, disk-like (oblate) and rod-like (prolate) spheroid micelles [6]. At higher concentrations, they can show a complex phase behavior of a range of liquid crystalline states [7]. Rhamnolipids display a similar solution behavior, but it is complicated by the carboxylic acid groups present that confer a pH dependence to these properties [8].

Chen et al. [9], have carried out a comprehensive neutron and light scattering study of the structure of R1, R2 and mixed R1 + R2 micelles, lamellar phase and vesicles. Single component R1 and R2 micelles best fitted an elliptical model, whilst mixed micelles of R1 + R2 were also elliptical but with a greater asphericity. Mixed micelles were also shown to have a high tendency to form vesicles or lamellar phases.

Given the emergence of biosurfactants, and rhamnolipids in particular, as functional molecules, there is a gap in knowledge concerning the functional properties of the various rhamnolipid congeners that differ in the number of rhamnose rings or lipid chain length and degree of unsaturation. The majority of information on surface activity of rhamnolipids with characterized structure concerns the R1 and R2 rhamnolipids, although there are multitudes of studies where the congener composition is not defined. The same structural features that control rhamnolipid micelle formation and structure will also influence the adsorption of the surfactants at air-water and oil-water interfaces. However, adsorption at an interface has not been studied in as much structural detail as micelle formation. Neutron reflectance has elucidated some of the features of R1 and R2 adsorption at oil-water interfaces [9], showing that they exhibit Langmuir adsorption type behavior. The area per molecule at the interface for R1 and R2 were determined as 60 and 75 $Å^2$ per molecule respectively [9]. The higher area per molecule for R2 relates to the larger volume occupied by the two rhamnose rings compared with one in R1. When R1 and R2 are present in mixtures, the R1 adsorbs preferentially to the interface due to the steric constraints on the R2 sugar head group.

If rhamnolipids are to be exploited fully in various industries for their functional properties a more detailed understanding of structure-functionality relationships is required such that the rhamnolipid congener with optimum functionality can be identified and selected for a particular application. In this study we use molecular dynamics simulation to probe the adsorption to the vacuum-water interface of R1, R2, a mono-rhamnolipid with two C14 alkanoate chains (C14C14), and two mixed alkyl chain mono-rhamnolipids (C14C10 and C10C14) and are thus of varied hydrophile-lipophile balance. Our aim is to facilitate the identification of rhamnolipid structural features that infer particular surface chemical and functionality attributes, and eventually to inform the directed selection of these biosurfactants for specific applications.

2. Methodology

Molecular dynamics simulation was used to model the adsorption of R1, R2, C14C14, C14C10 and C10C14 rhamnolipids in explicit water using a methodology we have reported previously [10,11]. The GROMACS molecular dynamics simulation program version 5 [12] was used for the simulations, with the GROMOS 54A7 force field [13]. The topology for the R1 and R2 structures (Fig. 1) and a mono-rhamnolipid with two C14 chains (C14C14), and mixed alkyl chains (C14C10, C10C14) were generated using the Automated Topology Builder [14–16]. Both non-ionic (i.e. protonated carboxyl group) and charged (dissociated carboxyl group) forms of the rhamnolipids were used. A single rhamnolipid was inserted into a cubic box of side length 5 nm and explicit SPCE water [17] was added to a total system density of 1000 gL^{-1}. Each simulation required approximately 4000 water molecules. A single sodium ion was added to each of the charged rhamnolipid systems to neutralize the charge of the ionized carboxyl group. Energy minimization was achieved using a conjugate gradients method [18].

The system was equilibrated for one ns in the NPT (isothermal-isobaric) ensemble using a Parrinello-Rahman barostat (1 bar) and a velocity-rescaling thermostat (300 K), during which time the box size is adjusted to equilibrate the pressure to one bar. The box size was then fixed at the average side length required to maintain one bar pressure, and the system equilibrated for 10 ns in the NVT canonical ensemble. The box size was increased to 15 nm in the z-dimension to create two water-vacuum interfaces. This setup with a single isolated rhamnolipid at an vacuum-water interface of approximately 5 nm^2 corresponds to the gas phase of the rhamnolipid surface pressure-area per molecule isotherm [19]. The systems were then run for 100 ns in the NVT ensemble to allow the rhamnolipids to adsorb at the vacuum-water interface, and a further 100 ns as the production run. The last 100 ns of the simulation were used for sampling, and conformations were taken every 10 ps (total of 10,000 conformations sampled). The particle mesh Ewald method [20,21] was used to sum the electrostatic components of the non-bonded interactions, with a cut off for both the coulombic and van der Waals interactions of 1 nm. The bonded interactions within a molecule were constrained using the LINCS algorithm [22].

Structural properties of the adsorbed rhamnolipid molecules were determined using GROMACS internal tools. The radius of gyration (R_g) of the rhamnolipids when at the interface was used to calculate the area occupied per molecule from the z-component of R_g parallel to the interface. The density of the rhamnose rings, alkyl chains, carboxyl group, and water phase was determined normal to the interface (z-direction). The radial water number density around the rhamnose, alkyl chains and carboxyl group was determined from the radial distribution function. This is defined as the radial distribution function normalised by radial number density. The head-group conformation was determined using a method proposed by Munusamy et al [23]. In this, the

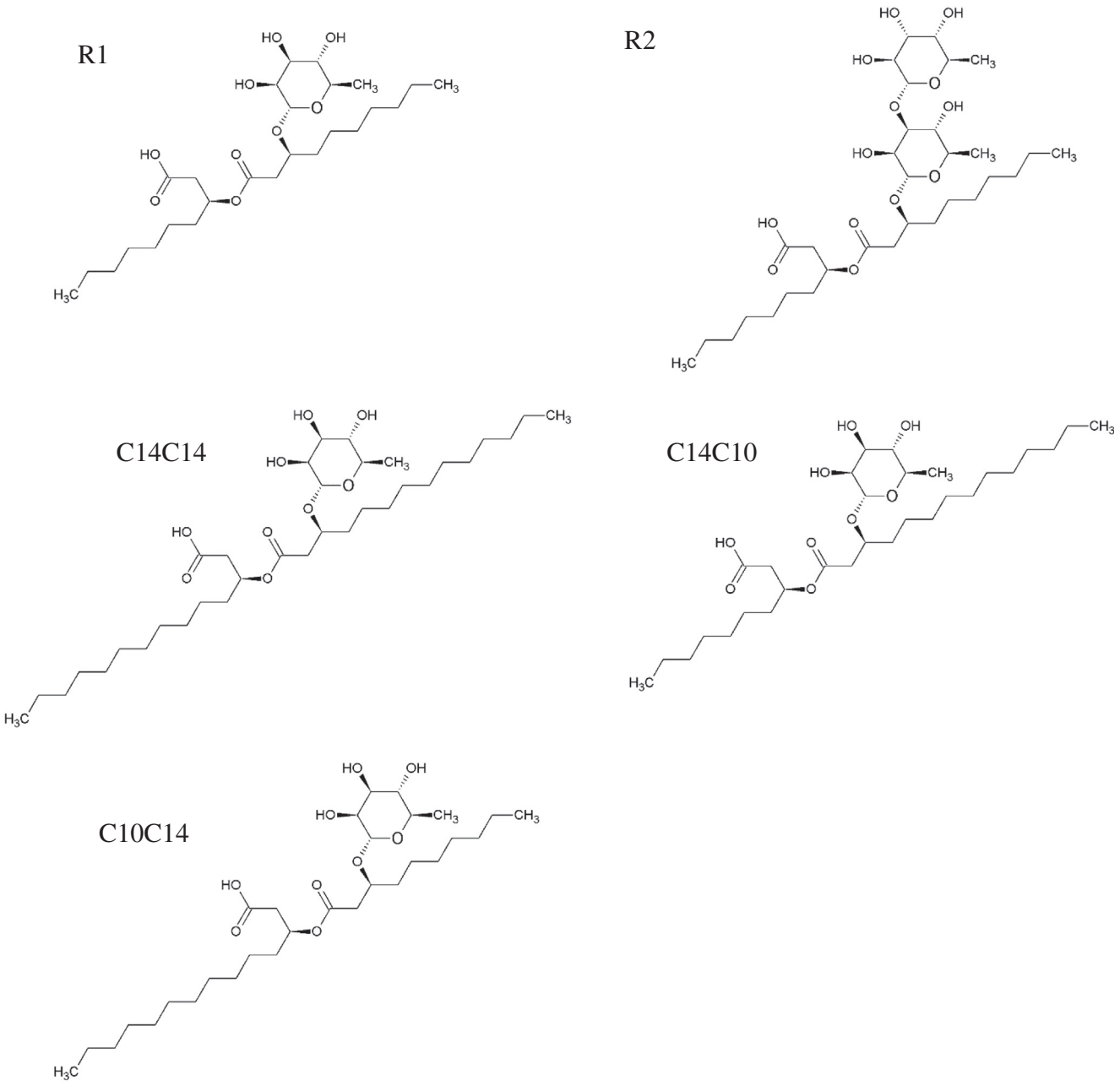

Fig. 1. Structures of the five rhamnolipids used in this study showing the designation of the alkyl 1 and alkyl 2 chains and of the two rhamnopyranose rings of R2.

shortest distance between the oxygens of the carboxyl group and any of the hydroxyl oxygens on the rhamnose ring is determined over the course of the simulation and the distribution function plotted. The tilt angle of the alkyl chain was measured as the angle between the vector from the carbon at the carboxyl end of the alkyl group and the terminal methyl and the normal to the interface. For the tilt angle, 0° indicates a chain aligned along the normal and upright at the interface, 90° is parallel (flat) to the interface and 180° is normal to the interface, but with the chain pointing towards or into the water phase. Lipid chain order parameters (S_{CD}) were calculated as the deuterium order parameter, defined by Eq. (1),

$$S_{CD} = \frac{1}{2}\left(3cos^2\langle\theta\rangle - 1\right) \quad (1)$$

with θ being angle between a bond in the alkyl chain and the normal to the vacuum-water interface (the z-axis). Finally, we use a method for estimating the free energy of adsorption that we have used previously for bile salts at vacuum-water and oil-water interfaces [10,11] and for proteins [24]. This involves umbrella sampling combined with the weighted histograms analysis method to define the potential of mean force for each of the rhamnolipids, from which the free energy of adsorption can be estimated. Harmonic wells spaced 0.2 nm apart were used to a range of 2 nm (a total of 14 wells/simulations), with a force constant of 1000 $kJ{\cdot}mol^{-1}{\cdot}nm^{-2}$ for each harmonic well. After the simulations for each well had completed, the histograms for each well were compared, and if there were any gaps in the coverage of the wells, simulations at intermediate spacings were run to improve coverage.

3. Results & discussion

3.1. Adsorbed conformations of rhamnolipid congeners

Fig. 2 shows typical snapshot adsorbed conformations for the different rhamnolipid congeners, both charged and uncharged. It is difficult to interpret these conformations as they represent a single snapshot in time, and not an ensemble average over 100 ns time as for the results that will be presented subsequently. However, it is clear that rhamnolipids can occupy a wide range of adsorbed conformations at the interface. They do, however, all show that the rhamnose rings are invariably closer to the water phase than the alkyl chains, which is a reflection of the amphiphilic nature of the rhamnolipid molecule.

3.2. Area occupied per molecule at the interface

Rhamnolipids are amphiphilic molecules, having a hydrophilic rhamnopyranose head group and largely hydrophobic alkanoate chains. Their structure is more complicated than many surfactants due to the presence of a terminal carboxyl group associated with the alkanoate chains that gives additional hydrophilic character and modifies adsorbed surfactant conformation. The area available for each rhamnolipid is approximately 2500 Å^2, indicating the rhamnolipids are highly dilute at the interface, and are in the gas-like phase of the area-surface pressure isotherm [19].

In practice, the physical area that the rhamnolipids occupy at the interface can be estimated from the z-component of the radius of gyration. The simulated R1, R2 and C14C14, C14C10 and C10C14 rhamnolipids have areas per molecule listed in Table 1. The values for R1 and R2 (both charged and uncharged) are close to the experimental values of 60 and 75 Å^2 per molecule reported by Chen et al. [9] for monolayers adsorbed at the air-water interface and estimated from the Gibbs equation. This suggests that the conformation is controlled by the overall hydrodynamic radius of the molecule, which does not change as the adsorbed layer packing density increases.

Experimental data for the other rhamnolipids is not available. Increasing the length of the alkyl chains, in general, increases the area occupied at the interface, with C14C14 having the largest values of 92 and 106 Å^2 in the uncharged and charged state. Clearly,

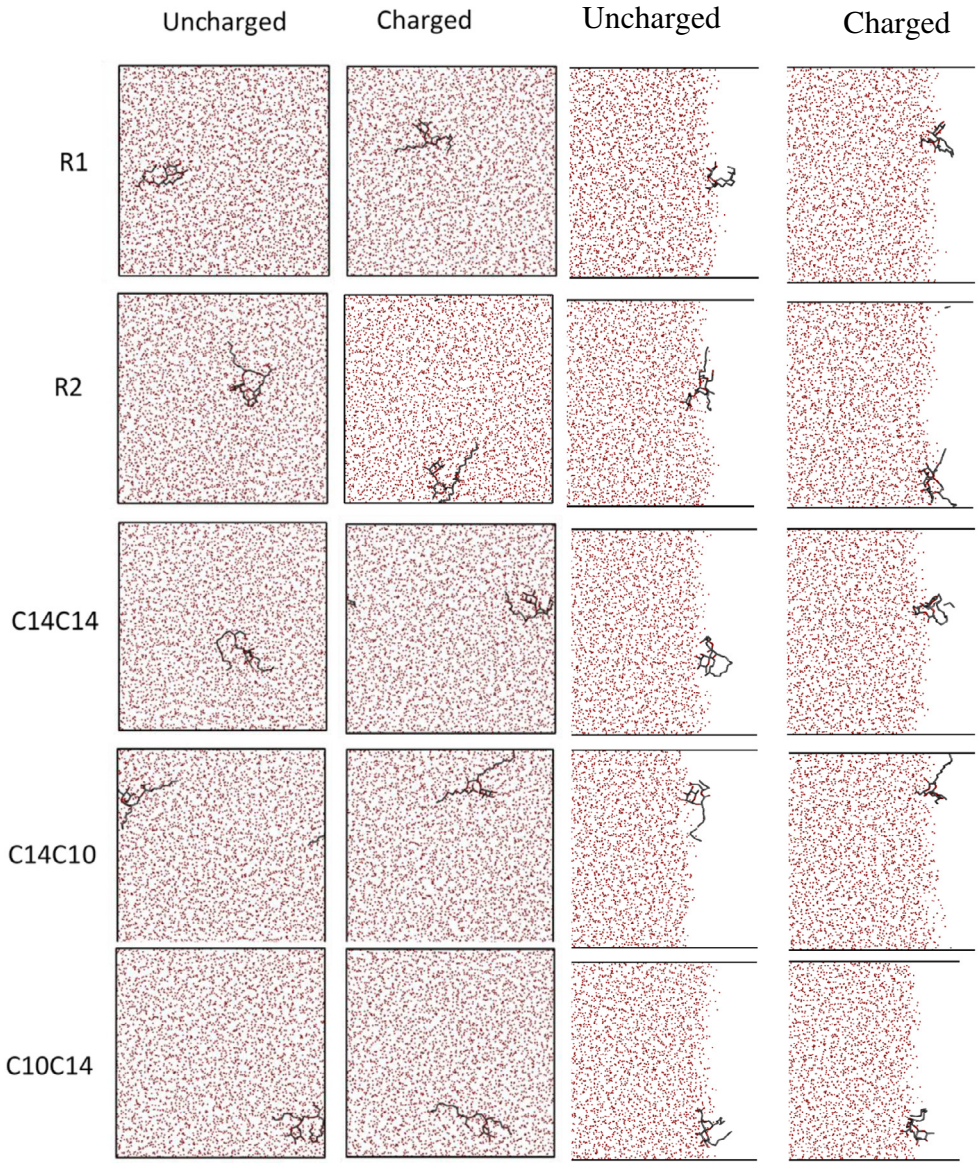

Fig. 2. Typical snapshot conformations for adsorbed charged and uncharged rhamnolipid congeners. Columns 1 and 2 are views from above the interface, whereas columns 3 and 4 are views across the interface.

Table 1
Area per molecule at the interface calculated from the z-component of the radius of gyration.

Rhamnolipid	Average area per molecule (Å^2)	
	Non-charged	Charged
R1	60 ± 14	61 ± 12
R2	73 ± 14	72 ± 10
C14C14	92 ± 29	106 ± 29
C14C10	80 ± 21	90 ± 17
C10C14	72 ± 22	86 ± 26

though, the position of the alkyl chains is important, as there is a significant difference between C10C14 and C14C10 rhamnolipids. The ionization state of the biosurfactant also changes the conformation at the interface, with an increased interfacial area observed for rhamnolipids in the charged state apart from for R1 and R2. Other simulation studies [25] have found that the surface area per molecule at the air-water interface is slightly higher (63.2 Å^2) for uncharged R1 than for charged R1 (57.2 Å^2) with this explained by interfacial rearrangement of the alkyl chain with the free carboxyl group.

3.3. Density profile of adsorbed rhamnolipids

Fig. 3 shows the density of the constituent parts (alkyl chains, carboxyl group, and rhamnopyranose ring) of the R1 rhamnolipid at the vacuum-water interface. Complementary figures for R2, C14C14, C14C10 and C10C14 rhamnolipids are in the supplementary material (Figure S1-S4). All parts of the rhamnolipids sit predominantly in the interfacial region where there is a decreasing density of the water phase. The rhamnolipids are oriented such that the alkyl chains sit predominantly on the vacuum side of the interface, the carboxyl groups closer to the bulk water phase, whilst the rhamnose rings sit across the interfacial region between. The rhamnopyranose and carboxyl groups penetrate further into the water phase, due to their greater ability to form hydrogen bonds with water. Theories for the conformation of adsorbed surfactants at air-water interfaces support these results, suggesting that alkyl chains should sit on the vacuum side of the interface, where they would not disrupt water-water H-bonding. This has been observed in other simulated adsorbed surfactant systems [10,11] where a substantial part of the hydrophobic regions of bile salts sit in the vacuum space. However, for rhamnolipids, the presence of the hydrophilic carboxyl group complicates this picture and clearly leads to significant adjustments to the alkyl chain conformation at the interface.

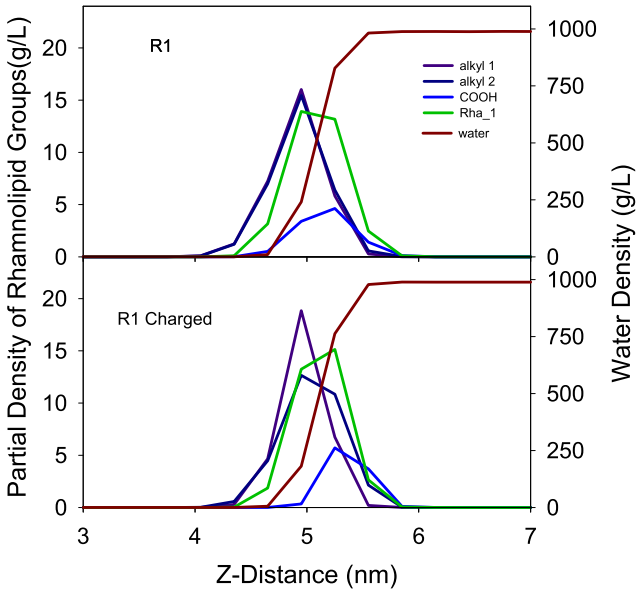

Fig. 3. Partial density profile for different functional groups in the R1 rhamnolipid at the vacuum-water interface.

For all simulated rhamnolipids, the non-ionized COOH group is strongly associated with the water phase and acts to anchor the alkyl chains to the water interface. The presence and position of the COOH group has the effect of drawing the alkyl chains closer to the water phase due to the formation of hydrogen bonds with the water molecules. This is likely to alter the conformation at the interface so that lipid chains are drawn closer to the water phase. This is exacerbated when the carboxyl group is ionized. In this case, the charged R1 carboxyl group is drawn further towards the water phase, causing a modest conformational rearrangement in the other groups (rhamnose ring and alkyl chains) which may have consequences for rhamnolipid surface activity. Abbassi et al. [25] have also seen that a simulated charged R1 molecule at the vacuum-water interface has carboxyl group that penetrates further into the water phase compared to the uncharged molecule. These trends in R1 conformation at the vacuum-water interface are also observed for the other rhamnolipid congeners. Chen et al. [9] deduced the density profiles for R1 and R2 at the air-water interface from a partial structure factor analysis of neutron reflectance data. They found that profiles for adsorbed R1 and R2 are essentially identical and that the larger R2 head group does not significantly alter the overall thickness of the adsorbed layer. This is in agreement with our simulation data in Fig. 3 and Figure S1 where we also observe little difference in the overall thickness of the adsorbed molecules, and little difference in distribution of the component groups of the surfactants.

3.4. Arrangement of water around rhamnolipid structural groups

The greater association of water to the carboxyl group and to the ionized carboxyl group in particular is clear from the water radial distribution function around the carboxyl of the R1 molecules (Fig. 4) and the other rhamnolipids (Supplementary figures S5-S8). For R1, a higher number of water molecules are associated with the carboxyl than other groups, with a clear hydration shell visible as a peak in the correlation function. Around the charged carboxyl group, the water is more ordered, with three peaks visible (Fig. 4) indicated a stratified, layered ordering of the water. There are less water molecules close to the alkyl chains compared to the rhamnopyranose rings and carboxyl group for all simulated rhamnolipids. This is also evident in the water radial distribution plots around the various functional groups of the other rhamnolipid molecules (Figures S5-S8).

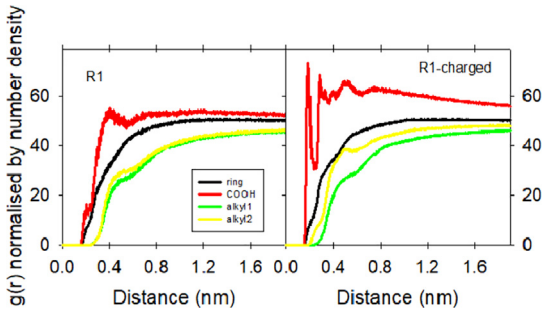

Fig. 4. The water radial distribution function normalized by radial number density around functional groups in the R1 rhamnolipid. Rha denotes the water number density around the rhamnose ring; COOH around the carboxyl; alkyl1 around alkyl chain 1; and alkyl2 around alkyl chain 2.

R1 and R2 adsorption at the vacuum-water interface has been simulated at more densely packed interfaces than we use in this study [26,27]. In these studies, little difference in the distribution of the alkyl chains at the interface between non-ionic and charged R1 is reported. It is also observed that the charged carboxyl group is better hydrated than the uncharged one, and that there is greater hydration of the rhamnose ring in the charged R1 molecule, which we did not observe in our results. For R2, the rhamnose ring 2 is better hydrated than ring 1 and the carboxyl group in R1 is more hydrated than in R2, although the alkyl chains for both R1 and R2 are distributed across the interface in a similar way for both R1 and R2 [27]. In our results, we also see little difference in the distribution of all groups across the interface for both R1 and R2. Taken together, these results suggest that there may be small differences between the density profiles for R1 and R2, but only at densely packed interfaces.

3.5. Head group conformation

To further probe the conformation adopted by the rhamnolipids at the vacuum-water interface, we have analyzed the head group conformation (minimum distance between carboxyl group and rhamnose ring) using the methodology suggested by Munsusamy et al. [26]. They found that charged and uncharged forms of R1 preferentially adopt one of four conformations that correspond to separations of approximately 0.3 nm (closed conformation), 0.6 and 0.8 nm (two partially open conformations) and 1.1 nm (open conformation). When the head group conformation was plotted over the course of a trajectory, it was found that in dense monolayers of uncharged R1 a closed conformation was adopted preferentially, with a second significant peak corresponding to the 0.8 nm partially open conformation and smaller contribution from the open conformation [26]. This distribution of head group conformations did not change significantly as the area per R1 molecule decreased (surface coverage increased) [26]. In contrast, the charged R1 molecule displayed a different head group distribution, where the closed conformation was absent, with the majority of conformations in a relatively wide peak centered on the partially open conformation at 0.6 nm, and also a slightly higher proportion of open conformations than the uncharged molecule [26]. They explained the absence of the closed conformation in the charged R1 as being due to this causing unfavorable interaction between and less effective packing of the alkyl chains at the interface.

For R2 Luft et al. [27] found that the ring attached to the alkyl chains (ring 1 in our work) interacts more strongly with the carboxyl group than ring 2. Unlike R1, where the head group adopts one of two conformations preferentially (closed or partially open) for R2, the closed conformation is highly preferred, which must be due to the presence of the second rhamnose ring. For our single isolated rhamnolipids that are adsorbed at a much lower surface coverage, we see a head group distribution that is different to that observed in a dense interfacial layer (Fig. 5). For most of our rhamnolipids in the non-charged form, there are roughly equal proportions of the closed (0.3 nm) and partially open (0.8 nm) conformations. The exception to this is the R2 di-rhamnolipid where the partially open conformation is favored over the closed conformation (the opposite of the situation observed at dense interfaces [27]) presumably due to a greater steric hindrance for the closed conformation due to the presence of the second rhamnopyranose ring.

We have also determined the distance between the carboxyl group and the second rhamnose ring for R2. This adopts a symmetrical distribution centered on 0.8 nm. For the charged rhamnolipids, all show an extremely strong preference for the closed conformation, presumably due to strong hydrogen bonding between the carboxyl and the rhamnose rings. This contrasts to the results in a dense monolayer [26] where the closed conformation was absent in the adsorbed charged R1, and so we would assume that for isolated rhamnolipids, unfavorable interactions and packing in the alkyl chains is not a factor in the adsorbed conformation.

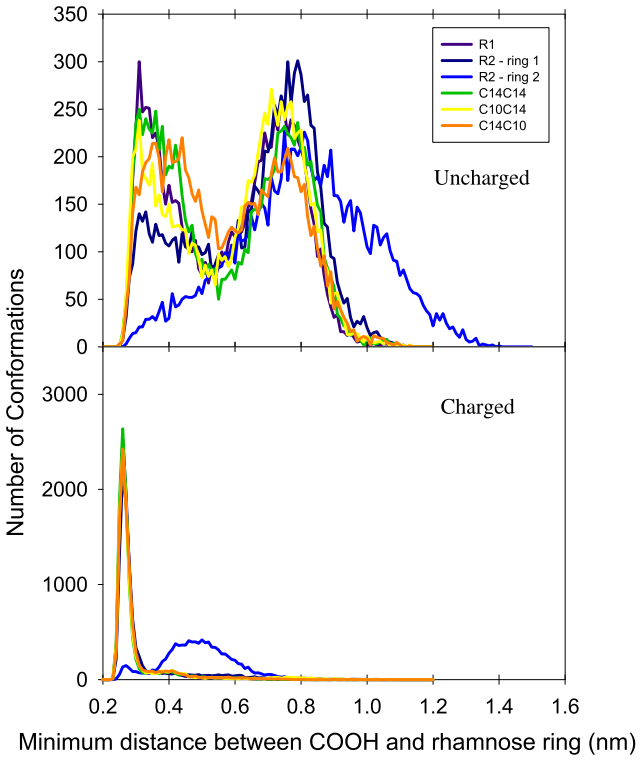

Fig. 5. Head group conformations for the five rhamnolipid congeners.

3.6. Alkyl chain tilt angle relative to the normal of the vacuum-water interface

Further information on the conformation of the rhamnolipids at the vacuum-water interface can be gained by looking at the orientation of the alkyl chains. The tilt angle for the alkyl chains (the angle between the normal to the interface and the vector between the first and last carbons of the alkyl chains) is shown in Fig. 6. For the uncharged rhamnolipids, alkyl chain 1 and 2 for R1, R2 and C14C14 and alkyl chain 1 for both C14C10 and C10C14 rhamnolipids all have average tilt angles between 70 and 80° indicating that on average they are close to flat on the interface (90°). The distribution around the average angle is, in general asymmetric with more conformations of tilt angle less than 70-80° showing a slight tendency for the alkyl chains to orient towards the vacuum phase. The exception to these observations is for the C14C10 and C10C14 rhamnolipid, where the second alkyl chain is oriented more towards the water phase and has a larger average tilt angle of 100° for the C10 in C14C10, and 110° for the C14 in C10C14. Clearly, having different length acyl chains has a greater effect on the orientation of alkyl chain 2 than increasing the chain length of both chains. A similar orientational preference of the alkyl chains of alcohols has been observed for simulations of various alcohol-water interfaces [28–30], with the alkyl chains being slightly tilted for alcohol molecules in the interfacial region and randomly oriented in the bulk.

This may be related to the extent of interaction between the two unequally sized chains compared to that which is possible

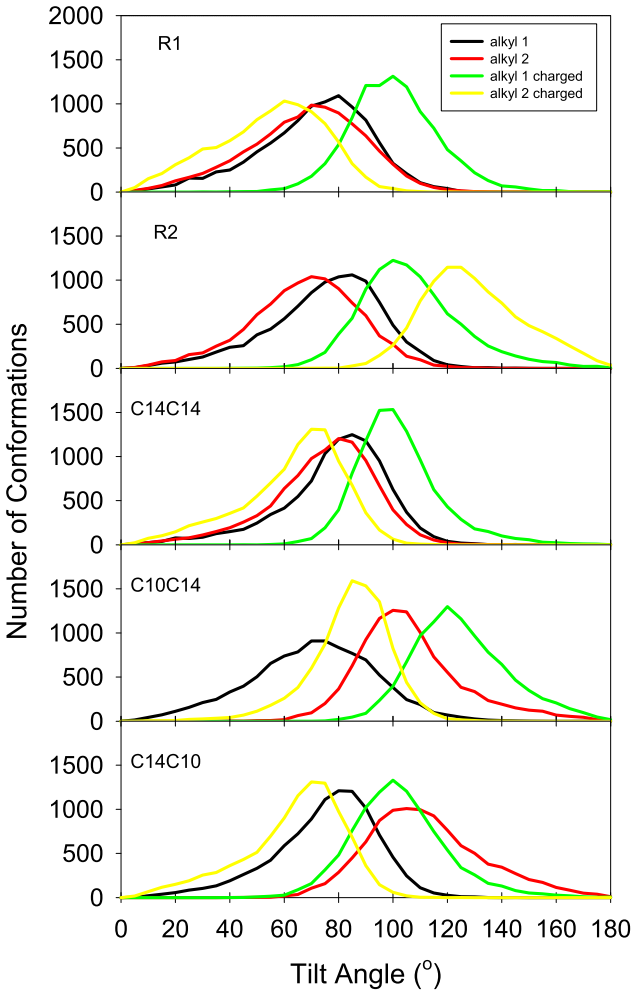

Fig. 6. Tilt angle distribution (angle between the vector defined by the two ends of the alkyl chains and the normal to the interface) for the five rhamnolipid congeners.

for two chains of the same size. Introducing a charge to the carboxyl group of the rhamnolipids has a significant effect on the tilt angle. In general, alkyl chain 2 (which has the carboxyl group at one end) increases in tilt angle, as the carboxyl is more strongly associated with the water phase, thus pulling alkyl chain 2 towards that phase. The exceptions to this are R2, where the average tilt angle of both alkyl chains increases, and C14C10 where the C14 (alkyl 1) tilt angle does not change significantly from the uncharged molecule, but the alkyl 2 chain tilts more towards the water phase. This suggests that the steric constraints of two rhamnolipids affects the alkyl chain orientation in R2, and the chain length position is important in determining tilt angle in rhamnolipids with unequal alkyl chains. For dense R1 and R2 interfaces [26,27] there is no difference between the tilt angles of the alkyl chains, which all have an angle of approximately 50°.

Experimental studies of the tilt angle of rhamnolipids at the interface are few. Wang et al. [19] have used polarization modulated-infrared reflection absorption spectroscopy (PMIRRAS) to study orientation of a C18C18 mono-rhamnolipid. They found that the tilt angle decreased as the monolayer density increased (decreasing area per molecule), and that the tilt angle did not change as pH (ionization state of carboxyl) changes, suggesting non-ionic and ionic forms would have very similar tilt angle. They hypothesize that tilt angle will not reach zero due to the geometry of head group packing.

3.7. Alkyl chain end-to-end length

The end-to-end length of the alkyl of chains can also be used to define the conformations at the vacuum-water interface. For a free polymer chain in solution the end to end distance of the chain can be approximated by a self-avoiding walk [31,32] as a scaling law with chain length, with the scaling coefficient dependent on chain interactions. For our rhamnolipids, a skewed distribution of end-to-end lengths is seen for all alkyl chains (Fig. 7). This is skewed to shorter end-to-end length since the chains are constrained at one end by being attached to a rhamnose ring or another alkyl chain and because the alkanoate chains interact through van der Waals forces. The end-to-end distribution is virtually identical for chains of the same size in all rhamnolipids (including mono and di-rhamnolipids) for both charged and uncharged carboxyl groups. Thus, the nature of the rhamnolipid (number of sugar rings) and the position of different sized alkyl chains does not influence the end-to-end distance this only being influenced by chain length.

3.8. Alkyl chain order parameter

The deuterium order parameter for the alkyl chains also indicates that there is very little ordering of the chains at the vacuum-water interface (Fig. 8). This is in agreement with the study of Brocca et al. [33] who probed the structure of a mono-rhamnolipid layer in the gas state using a pendant drop coupled

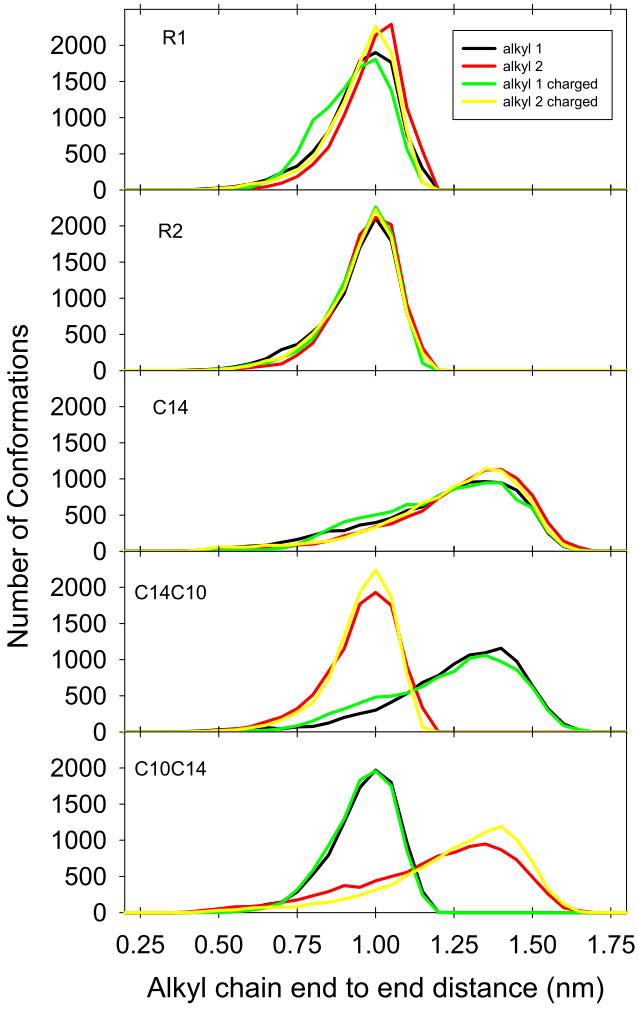

Fig. 7. Alkyl chain end-to-end distance for the five rhamnolipid congeners.

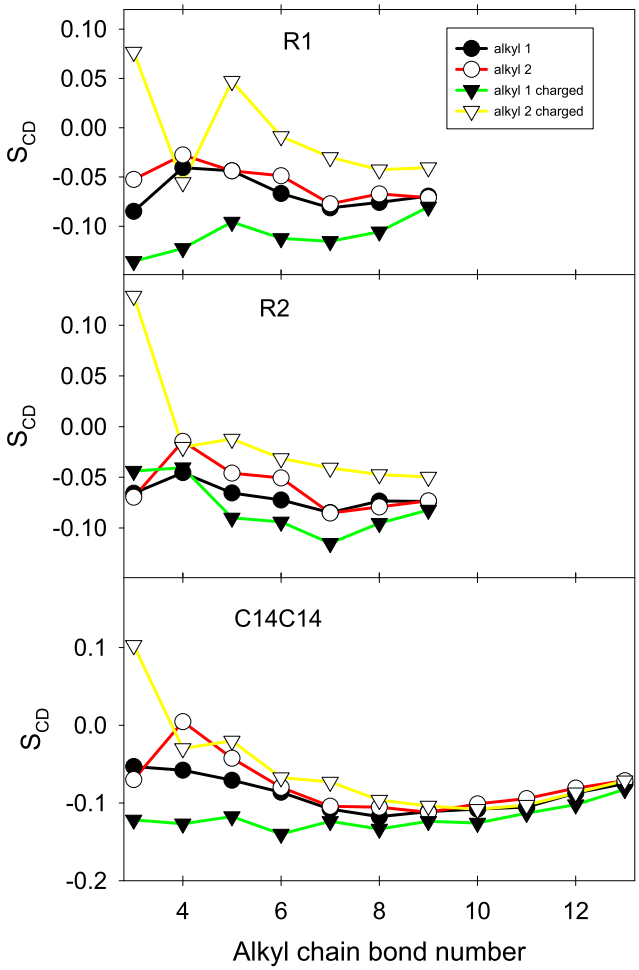

Fig. 8. Alkyl chain order parameter for the five rhamnolipid congeners.

to a differential interferometric detector allowing surface tension measurements at low concentrations. They found no orientational order of the mono-rhamnolipid monolayer in the gas state.

3.9. Free energy of adsorption

The affinity of the different rhamnolipids to the vacuum-water interface is reflected in the computationally determined free energy of adsorption, which is presented in Table 2. For uncharged rhamnolipids, the free energy of adsorption varies little between the different congeners, with only C14C14 significantly more strongly bound to the interface than the other rhamnolipids, probably because of its greater overall hydrophobicity. The charged congeners show a greater variation in the free energy of adsorption. Charged congeners are more strongly bound to the interface (more negative ΔE_{ads}) apart from R1 and R2, which have a less negative free energy of adsorption. For the charged congeners, C14C14 again has a high adsorption energy, but also the C10C14 congener shows a much higher adsorption energy in its charged state.

Table 2
Free energy of adsorption calculated using umbrella sampling.

Rhamnolipid	ΔEads (kJ·mol^{-1})	
	Uncharged	Charged
R1	−54.0 ± 0.6	−50.8 ± 0.5
R2	−55.6 ± 0.3	−43.8 ± 0.5
C14C14	−58.6 ± 0.4	−66.6 ± 1.3
C14C10	−54.0 ± 1.2	−57.6 ± 1.2
C10C14	−54.7 ± 1.0	−62.6 ± 0.7

3.10. General discussion

The modelling studies here show that there are differences in the conformations adopted by the various rhamnolipids at the vacuum-water interface, although most of these are relatively small. We might expect these differences to translate into altered surface-active properties for the rhamnolipids, although given the subtle nature of the conformational changes the effect on surface activity may be small. The effect of rhamnolipid structure and charge state of the carboxyl group clearly affects the adsorption of the different congeners, but the precise relationship between structure and adsorption is complex. There are very few experimental studies on the surface activity of rhamnolipids other than for R1 and R2. Fernández-Peña et al. [34] measured the adsorbed amount of four rhamnolipids on to a negatively charged quartz crystal surface. They found that the total adsorbed amount changed in the order di-RL(C14) > mono-RL(C10) > di-RL(C10) with mono-RL(C14) having too low solubility in water to allow measurement, with the data reflecting the higher hydrophobicity of rhamnolipids with one sugar ring and longer alkyl chains.

A number of researchers have measured the surface tension profile for R1 and R2. Chen et al. [9] measured surface tension at water pH 7 and pH 9 buffers and 0.5 M NaCl –air interfaces. R1 did lower the surface tension more than R2 at concentrations below the CMC but only by a modest 3–6 mN.m^{-1}. Ikizler et al. [35] also observed that R1 lowers surface tension more than R2. Altering the charge on both R1 and R2 has also been observed to lead to changes in surface tension [36,37]. Increasing the NaCl concentration up to 1 M [36] screens the charge on the carboxyl group and reduces the surface tension of both R1 and R2 (at concentrations below the CMC) by up to 10 mN·m^{-1}. Similarly, lowering the pH from 6.8 to 5, which neutralizes the charge on the carboxyl group also leads to a reduction in surface tension for both R1 and R2 [37]. Abbassi and co-workers [25] also observed a decrease in surface tension measured experimentally on lowering the pH of R1 solutions from 7 to 4, and correlated this with molecular dynamics simulations where there was a change in the distribution of the carboxyl group at the interface when it is charged.

4. Conclusions

Rhamnolipids are produced as mixed congers in microbial fermentations, although often a few congeners predominate. In the absence of experimental data on the surface behavior of the majority of rhamnolipid congeners produced by bacteria it is not possible to determine which, if any of the congeners has superior surface chemical properties and would be desirable to over-produce in fermentations. Computer simulation offers an alternative way to assess biosurfactant properties to throw light on the factors influencing their surface chemistry. We have found that all rhamnolipid congeners studied adsorb with the sugar rings oriented to the water and the lipid chains to the vacuum phase. However, the conformation adopted differs depending on congener type. The congener head group conformation shows two preferred orientations, a closed conformation where the carboxyl group is 0.3 nm from the sugar ring and an open conformation where this distance is 0.8 nm. Uncharged congeners have approximately equal distribution of the two orientations apart from the di-rhamnolipid where steric hindrance from the second rhamnose ring presumably leads to a preference for the partially open conformation. In charged congeners, stronger interaction between the ionized carboxyl group and the hydroxyl groups of the sugar rings gives a very

strong preference for the closed conformation, apart from for the di-rhamnolipid, where it is presumed that steric hindrance limits the proportion of closed congeners. Differences are also observed for the orientation of the lipid chains amongst congeners, particularly those with unequal acyl chain lengths. Lipid chains chain order parameters show these are disordered at the interface. The tilt angle is similar for all alkyl chains in those congeners with equal carbon chain length (irrespective of whether they are C10 or C14 chains) but if they are unequal, one chain has a greater probability of tilting towards the water phase. The presence of a charge on the carboxyl group also changes the distribution of acyl chain tilt angles in each conger but does not alter the alkyl chain end-to-end distance distribution. All told, these results support our hypothesis that molecular dynamics simulation can be used to differentiate between the adsorption properties of rhamnolipid congeners at a vacuum-water interface.

The simulation results are in general agreement with the sparse experimental data for different rhamnolipid congeners that is available in the literature [9,25,34–37], and support and expand the range of reported simulations on adsorbed conformation of rhamnolipids [26,27]. Although our work is a starting point to understand potential differences in the adsorption and surface chemistry of rhamnolipid congeners, we have to recognize that a single isolated adsorbed rhamnolipid will not fully represent the adsorption behavior of these molecules, as in practice they will be adsorbed in a close-packed monolayer where the behavior of individual surfactants will be influenced by interaction with others surrounding them. Therefore, a natural extension of this work is to simulate at concentrated biosurfactant interfaces as a more realistic model system.

Our observations also suggest that it would be worthwhile selectively extracting a range of rhamnolipid congeners to understand better their adsorption properties. This would allow a more informed selection of these as industrial chemicals, enabling the properties of these surfactants to be tailored to a particular application.

CRediT authorship contribution statement

Stephen R. Euston: Conceptualization, Formal analysis, Funding acquisition, Investigation, Writing-original draft. **Ibrahim M. Banat**: Funding acquisition, Writing – review and editing. **Karina Salek**: Writing – review and editing.

Declaration of Competing Interest

The authors declare that they have no known competing financial interests or personal relationships that could have appeared to influence the work reported in this paper.

Acknowledgment

This study was supported by the European Union's Horizon 2020 Research and Innovation Programme under Grant Agreement No. 635340 (MARISURF).

Appendix A. Supplementary material

Supplementary data to this article can be found online at https://doi.org/10.1016/j.jcis.2020.11.082.

References

[1] I.M. Banat, A. Franzetti, I. Gandolfi, G. Bestetti, M.G. Martinotti, L. Fracchia, T.J. Smyth, R. Marchant, Microbial biosurfactants production, applications and future potential, Appl. Microb. Technol. 87 (2010) 427–444.
[2] I. Klosowska-Chomiczewska, K. Medrzycka, E. Karpenko, Biosurfactants–biodegradability, toxicity, efficiency in comparison with synthetic surfactants, in: Proceedings of the Polish-Swedish-Ukrainian Seminar Research and Application of New Technologies in Wastewater Treatment and Municipal Solid Waste Disposal in Ukraine, Sweden, and Poland, Krakow, 2011, p. 1.
[3] K. Salek, S.R. Euston, Sustainable microbial biosurfactants and bioemulsifiers for commercial exploitation, Process Biochem. 85 (2019) 143–155.
[4] I.M. Banat, R.S. Makkar, S.S. Cameotra, Potential commercial applications of microbial surfactants, Appl. Microb. Technol. 53 (2000) 495–508.
[5] T.F. Tadros, in: Phase Behavior of Surfactant Systems Applied Surfactants: Principles and Applications, Wiley-VCH Verlag GmbH & Co, KGaA, Weinheim, 2005, p. 53.
[6] O. Söderman, I. Johansson, Polyhydroxyl-based surfactants and their physicochemical properties and applications, Curr. Opinion Colloid Interface Sci. 4 (2000) 391–401.
[7] T. Imura, Y. Hikosaka, W. Worakitkanchanakul, H. Sakai, M. Abe, M. Konishi, H. Minamikawa, D. Kitamoto, Aqueous phase behavior of natural glycolipid biosurfactant, mannosylerythritol lipid-a: sponge, cubic, and lamellar phases, Langmuir 23 (2007) 1659–1663.
[8] Y. Ishigami, Y. Gama, H. Nagahora, M. Yamaguchi, H. Nakahara, T. Kamata, The-pH sensitive conversion of molecular aggregates of rhamnolipid biosurfactant, Chem. Lett. 16 (1987) 763–766.
[9] M.L. Chen, J. Penfold, R.K. Thomas, T.J.P. Smyth, A. Perfumo, R. Marchant, I.M. Banat, P. Stevenson, A. Parry, I. Tucker, I. Grillo, Solution self-assembly and adsorption at the air-water interface of the mono-rhamnose and di-rhamnose rhamnolipids and their mixtures, Langmuir 26 (2010) 18281–18292.
[10] S.R. Euston, U. Bellstedt, K. Schillbach, P.S. Hughes, The adsorption and competitive adsorption of bile salts and whey protein at the oil–water interface, Soft Matter 7 (2011) 8942–8951.
[11] S.R. Euston, W.G. Baird, L. Campbell, M. Kuhns, Competitive adsorption of dihydroxy and trihydroxy bile salts with whey protein and casein in oil-in-water emulsions, Biomacromolecules 14 (2013) 1850–1858.
[12] M.J. Abraham, T. Murtola, R. Schulz, S. Páll, J.C. Smith, B. Hess, E. Lindahl, GROMACS: High performance molecular simulations through multi-level parallelism from laptops to supercomputers, SoftwareX 1–2 (2015) 19–25.
[13] N. Schmid, A.P. Eichenberger, A. Choutko, S. Riniker, M. Winger, A.E. Mark, W.F. van Gunsteren, Definition and testing of the GROMOS force-field versions 54A7 and 54B7, Eur. Biophys. J. 40 (2011) 843.
[14] A.K. Malde, L. Zuo, M. Breeze, M. Stroet, D. Poger, P.C. Nair, C. Oostenbrink, A.E. Mark, An Automated force field Topology Builder (ATB) and repository: Version 1.0, J. Chem. Theory Comput. 7 (2011) 4026–4037.
[15] S. Canzar, M. El-Kebir, R. Pool, K. Elbassioni, A.K. Malde, A.E. Mark, D.P. Geerke, L. Stougie, G.W. Klau, Charge group partitioning in biomolecular simulation, J. Comput. Biol. 20 (2013) 188–198.
[16] K.B. Koziara, M. Stroet, A.K. Malde, A.E. Mark, Testing and validation of the Automated Topology Builder (ATB) version 2.0: Prediction of hydration free enthalpies, J. Comput. Aided Mol. Des. 28 (2014) 221–233.
[17] H.J.C. Berendsen, J.R. Grigera, T.P. Straatsma, The missing term in effective pair potentials, J. Phys. Chem. 91 (1987) 6269–6271.
[18] M.R. Hestenes, E. Stiefel, Methods of conjugate gradients for solving linear systems, J. Res. Nat. Bur. Stand. 49 (1952) 411–436.
[19] H. Wang, C.S. Coss, A. Mudalige, R.L. Polt, J.E. Pemberton, A PM-IRRAS investigation of monorhamnolipid orientation at the air–water interface, Langmuir 29 (2013) 4441–4450.
[20] T. Darden, D. York, L. Pedersen, Particle mesh Ewald: an N· log (N) method for Ewald sums in large systems, J. Chem. Phys. 98 (1993) 10089–10092.
[21] U. Essmann, L. Perera, M.L. Berkowitz, T. Darden, H. Lee, L. Pedersen, A smooth particle mesh Ewald method, J. Chem. Phys. 103 (1995) 8577–8593.
[22] B. Hess, H. Bekker, H.J.C. Berendsen, J.G.E.M. Fraaije, LINCS: a linear constraint solver for molecular simulations, J. Comput. Chem. 18 (1997) 1463–1472.
[23] E. Munusamy, C.M. Luft, J.E. Pemberton, S.D. Schwartz, Structural properties of nonionic monorhamnolipid aggregates in water studied by classical molecular dynamics simulations, J. Phys. Chem. B 2017 (121) (2017) 5781–5793.
[24] H.A. Alghamdi, L.J. Campbell, S.R. Euston, Molecular dynamics simulation of the adsorption of mung bean defensin VrD1 to a phospholipid bilayer, Food Struct. 21 (2019) 100117.
[25] H. Abbasi, K.A. Noghabi, M.M. Hamedi, H.S. Zahiri, A.A. Moosavi-Movahedi, M. Amanlou, J.A. Teruele, A. Ortiz, Physicochemical characterization of a monorhamnolipid secreted by Pseudomonas aeruginosa MA01 in aqueous media. An experimental and molecular dynamics study, Colloids Surf., B 101 (2013) 256–265.
[26] E. Munusamy, C.M. Luft, J.E. Pemberton, S.D. Schwartz, Unraveling the differential aggregation of anionic and nonionic monorhamnolipids at air–water and oil–water Interfaces: a classical molecular dynamics simulation study, J. Phys. Chem. B 122 (2018) 6403–6416.
[27] C.M. Luft, E. Munusamy, J.E. Pemberton, S.D. Schwartz, A classical molecular dynamics simulation study of interfacial and bulk solution aggregation properties of dirhamnolipids, J. Phys. Chem. B 124 (2020) 814–827.
[28] I. Benjamin, Polarity of the water/octanol interface, Chem. Phys. Lett. 393 (2004) 453–456.
[29] P. Jedlovszky, I. Varga, T. Gilányi, Adsorption of 1-octanol at the free water surface as studied by Monte Carlo simulation, J. Chem. Phys. 120 (2004) 11839–11851.

[30] J. Algaba, J.M. Míguez, P. Gómez-Álvarez, A. Mejía, F.J. Blas, Preferential orientations and anomalous interfacial tensions in aqueous solutions of alcohols, J. Phys. Chem. B 124 (2020) 8388–8401.
[31] P.H. Verdier, W.H. Stockmayer, Monte Carlo calculations on the dynamics of polymers in dilute solution, J. Chem. Phys. 36 (1962) 227–235.
[32] J. Mazur, Distribution function of the end-to-end distances of linear polymers with excluded volume effects, J. Res. Natl. Bureau Standards: Sect. A Phys. Chem. 69 (1965) 355–363.
[33] P. Brocca, V. Rondelli, M. Corti, E. Del Favero, M. Deleu, L. Cantu, Interferometric investigation of the gas-state monolayer of mono-rhamnolipid adsorbing at an oil/water interface, J. Mol. Liq. 266 (2018) 687–691.
[34] L. Fernández-Peña, E. Guzmán, F. Leonforte, A. Serrano-Pueyo, K. Regulski, L. Tournier-Couturier, F. Ortega, R.G. Rubio, G.S. Luengo, Effect of molecular structure of eco-friendly glycolipid biosurfactants on the adsorption of hair-care conditioning polymers, Colloids Surf. B: Biointerfaces 185 (2020) 110578.
[35] B. İkizler, G. Arslan, E. Kipcak, C. Dirik, D. Çelenk, T. Aktuğlu, Ş.Ş. Helvacı, S. Peker, Surface adsorption and spontaneous aggregation of rhamnolipid mixtures in aqueous solutions, Colloids Surf., A 519 (2017) 125–136.
[36] Ş.Ş. Helvacı, S. Peker, G. Özdemir, Effect of electrolytes on the surface behavior of rhamnolipids R1 and R2, Colloids Surf. B: Biointerfaces 35 (2004) 225–233.
[37] G. Özdemir, S. Peker, S.S. Helvaci, Effect of pH on the surface and interfacial behavior of rhamnolipids R1 and R2, Colloids Surf., A 234 (2004) 135–143.